

Isotopic dependence of (n, α) reaction cross sections for Fe and Sn nuclei

S. Küçüksu^a, M. Yiğit^b, N. Paar^a

^aDepartment of Physics, Faculty of Science, University of Zagreb, Bijenička c. 32, Zagreb, 10000, Croatia

^bDepartment of Physics, Faculty of Arts and Science, Aksaray University, Aksaray, 68100, Türkiye

Abstract

The (n, α) reactions play an important role for the energy generation and the synthesis of chemical elements in the stars, as well as for nuclear engineering and medical applications. The aim of this study is to explore the evolution of (n, α) reactions in Fe and Sn isotope chains in order to assess the cross section properties with the increase of neutron number in target nucleus, and to make a comparison with other relevant neutron induced reactions. The cross section calculations are based on the statistical Hauser-Feshbach and exciton models in TALYS nuclear reaction code, using global optical model potential that is additionally adjusted by the (n, α) cross section data for ^{54}Fe and ^{118}Sn . The calculations of (n, α) reactions in Fe and Sn isotopes provide the insight into their isotopic dependence and properties over the complete relevant range of neutron energies. The cross sections result in pronounced maxima at lower-mass isotopes, and rather strong decrease for neutron-rich nuclei consistent with the reduction of the reaction Q -value and increased contributions from other exit channels from compound nucleus. The analysis of the Maxwellian averaged cross sections at temperatures in stellar environment shows that the (n, α) reactions have significant contributions for low-mass Fe isotopes, that is opposite than for Sn isotopes. For both neutron rich isotopes γ and neutron emissions dominate, with their interplay depending on the temperature involved.

1. Introduction

Neutron induced nuclear reactions are essential in stellar nucleosynthesis, nuclear engineering and medical applications. The synthesis of elements heavier than Iron is governed mainly by (i) slow neutron capture process (s-process) in giant stars [52] and rotating massive metal poor stars [10] and (ii) rapid neutron capture process (r-process) occurring in explosive stellar environments such as supernovae [92] and in neutron star mergers [27]. There are also other neutron capture processes like the i-process, at neutron densities between those of s- and r- process, suggested to explain part of the observed heavy element abundances [41]. In many astrophysical conditions (n, γ) reactions play a dominant role, however other neutron induced reactions also participate, including the (n, α) reaction. In the interplay with nuclear β -decay, these reactions determine the path of the nucleosynthesis processes. Since the (n, α) reaction may also contribute, it is interesting to explore in more details the properties of this reaction in comparison to other competitive reactions.

The (n, α) reactions have recently been investigated experimentally due to their role in nucleosynthesis, especially related to the s-process, e.g. in Refs [74, 22, 31, 34, 93, 96, 26, 11, 32, 80, 9, 44, 61]. The (n, α) reaction has also been recently studied for ^7Be target, to

address the cosmological lithium problem using the measurement of the reaction cross section in a wide energy range [11]. Novel experimental techniques and detector systems have been recently developed to provide accurate new data [95, 39]. Recent developments also include the NICE-detector, that opened new perspectives to determine neutron capture cross sections with charged particle in the exit channel with sufficient accuracy, for different nuclear and astrophysical applications [3]. The studies of (n, α) reactions are also important due to their possible medical applications. For example, in the Boron Neutron Capture Therapy (BNCT) of cancer, Boron-10 is irradiated with low-energy thermal neutrons to yield high linear energy transfer particles and recoiling Lithium-7 nuclei [12]. Recently, ^{33}S has been studied as a cooperating target for the BNCT because of its large (n, α) cross section in the epithermal neutron energy range, that is the most suitable for the BNCT [86]. Further studies are needed for complete description of the (n, α) reactions on various nuclear targets relevant in medical applications.

From the experimental side, the properties of (n, α) reactions remain unknown for many nuclei or they are available in restricted neutron energy ranges [81]. Therefore, theoretical description is indispensable to provide complete knowledge on the cross sections relevant for many applications. Reaction theory of neutron capture in nuclei crucially depends on the nuclear structure and excitation properties of target and daughter nuclei involved [64]. Since theoretical approaches to (n, α) reactions

Email addresses: semak@phy.hr (S. Küçüksu), npaar@phy.hr (N. Paar)

are subject to systematic uncertainties in various nuclear properties involved, reliable description of (n, α) reaction cross sections requires both theoretical modelling and advanced experimental methods. The nuclear reaction cross sections, both from the experiment and model calculations are available in several data bases, e.g. in Refs. [74, 18, 85, 78, 89, 4, 30]. Although some analyses are available on the isotopic dependence of neutron induced reactions, often they are rather limited, e.g., based on simple phenomenological formula constrained by experimental data [99]. Since the experimental data are often limited in terms of the incoming neutron energy, reaction theory approaches are essential to provide the insight how the neutron induced reaction cross sections evolve along the nuclide map. The advent of modern and complete nuclear reaction theory frameworks (e.g., TALYS [58, 59], EMPIRE[45], NON-SMOKER [85], etc.), opened perspective to investigate in detail how specific neutron induced reaction cross sections over the broad neutron energy range evolve when going away from the valley of stability.

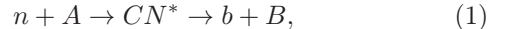
The aim of this work is to investigate theoretically the (n, α) reaction cross sections along two representative isotope chains, Fe and Sn, in order to understand how the cross sections evolve with increasing neutron number of target nucleus. The experimental data on ^{54}Fe will be used to benchmark model calculations for their extension toward neutron rich isotopes. In order to assess the relevance of (n, α) reactions in stellar environment, neutron induced reactions with several exit channels will be explored and compared. For this purpose, also Maxwellian averaged cross sections (MACS) will be calculated, assuming Maxwell-Boltzmann distribution of the incoming neutron flux. Model calculations will be performed using Hauser-Feshbach statistical model [43, 72] and its implementation in the nuclear reaction program TALYS [58, 59]. This framework represents one of the most advanced approaches to describe nuclear reactions, and it also provides the overview of the systematic uncertainties due to various inputs on nuclear structure and reaction properties.

The paper is organized as follows. Section 2 includes a brief description of the theory framework and settings used for modelling (n, α) and other neutron-induced reactions of interest and its implementation in the TALYS code. In Sec. 3.1 the results on the benchmark calculation for ^{54}Fe in comparison to the experimental data are shown. In addition, the results on the analysis of isotopic dependence of (n, α) reaction cross sections are presented in Sec. 3.1 and Sec. 3.2 for Fe and Sn isotopes, respectively. Section 3.3 includes the corresponding analysis of the MACS values. Summary and conclusions of the present work are given in Sec. 4.

2. Theory framework

Compound nucleus reactions induced with neutrons are investigated in the framework of statistical Hauser-Feshbach model, while pre-equilibrium reaction process is

described by excitation model, both in their computational implementation in the reaction code TALYS [58, 59]. Here we give only a brief overview of the framework settings used in this work, for more details see Ref. [59]. Statistical model is employed to describe the binary reaction [46]



where the projectile is incoming neutron (n), A denotes target, CN^* excited intermediate compound nucleus, b is ejectile and B the residual nucleus. The interaction between neutron and target nucleus A is described by the effective (optical) potential and the reaction problem is solved numerically [46]. While the incident channel is determined by neutrons, many outgoing reaction channels are possible. The compound nucleus reaction cross sections can be described using statistical Hauser-Feshbach model [43, 72, 85]. It assumes the validity of the compound nucleus reaction mechanism and a statistical distribution of nuclear excited states [72, 52]. However, there are limitations for its application, so the method is appropriate when the level density in the contributing energy window around the peak of the projectile energy distribution is sufficiently high to justify a statistical treatment [85]. For the energy of incident particle below ≈ 20 MeV, the compound nucleus reaction dominates. At intermediate energies, additional contributions are possible through the pre-equilibrium reaction process, that is described by the exciton model [59]. There are many possible exit channels with various outgoing particles, where the dominant contributions come from neutron, γ -ray, proton, and α -particle. The (n, α) reaction cross sections have been previously investigated with the Hauser-Feshbach model in calculations of astrophysical reaction rates for large set of nuclei [85].

For the purpose of the present work, the Hauser-Feshbach and exciton models, implemented in the TALYS code [58, 59] are used to investigate the isotopic dependence of (n, α) reaction cross sections over the broad energy range up to ≈ 20 MeV, including also a comparison with the cross sections for several other relevant exit channels. More details about relevant nuclear structure properties included in the model are given in Ref. [59]. The reaction cross sections sensitively depend on the nuclear level densities, as well as on the optical model transmission coefficients [59]. The properties of target nuclei can be used from available experimental data or theoretical models. Since the present study includes isotopic chains for which experimental data are limited, only theoretical description can provide all necessary quantities. Phenomenological models are often used instead of experimental data [85]. In this work, the Skyrme functional is used for the description of nuclear masses, [35]. In this way, important input for nuclear reaction study is determined from global microscopic model.

The Hauser-Feshbach model also requires description of

the transmission coefficients for the α particle emission. In this work we employ well established global optical model potential from Ref. [56], where the parameterisation used is given in the TALYS implementation [59]. However, since the measured (n, α) cross sections could not be accurately described for two benchmark nuclei in this study, ^{54}Fe and ^{118}Sn , additional adjustments of the optical model potential has been performed. More details about this procedure are given in Sec. 3.1. Compound nucleus cross section also includes width fluctuation correction (WFC) which accounts for the correlations between the incident and outgoing waves [59]. These correlations enhance the elastic channel, and accordingly decrease other open channels. In this work the WFC factors are calculated using standard implementation of the Moldauer model [71]. For the level densities, Back-shifted Fermi gas Model (BFM) is used [23], that fits the best the experimental data of interest in this work. At intermediate incoming neutron energies the pre-equilibrium reaction channels start to open. Thus, for the comparison of the model calculations with experimental data, we also include pre-equilibrium process in theory framework. For the calculations of pre-equilibrium reactions, the exciton model is used [57]. With these settings, we use the TALYS code [59] to investigate the (n, α) reaction cross sections, as well as the Maxwellian averaged cross sections (MACS) at temperatures characteristic in stellar environments.

3. Isotopic dependence of (n, α) reaction cross sections

By employing the nuclear reaction framework and its computational implementation outlined in Sec. 2, in the following we investigate the evolution of the properties of (n, α) reaction cross sections in two representative isotope chains - Fe and Sn. In addition, for comparison we also perform more systematic analysis including other relevant exit channels, including neutron, proton, and γ emission.

3.1. Fe isotopes

First we consider model calculations for ^{54}Fe , because it is the only Fe isotope with available systematic experimental data on (n, α) reaction cross sections covering a broad range of the incoming neutron energies up to ≈ 18 MeV [76, 68, 69, 67, 94, 37, 42, 88, 87, 54, 20, 66, 48]. Therefore, we choose ^{54}Fe for benchmarking the settings of the nuclear reaction model for further studies in Fe isotopes. Since we aim to study the systematics of the cross sections along isotope chains for (n, α) reactions, the most appropriate are the implementation of the global optical model potential of Koning and Delaroche [56] and alpha optical model from Avrigeanu et al. [8] as outlined in Ref. [59]. The α -nucleus optical potential is usually constrained by employing data from elastic alpha scattering experiments [53, 47, 24, 7, 70, 75]. In order to improve description of experimental data for (n, α) cross sections

for ^{54}Fe [76, 68, 69, 67, 94, 37, 42, 88, 87, 54, 20, 66, 48], a rescaling of the optical model potential mass dependent geometry parameters for radius r_v, r_w , for diffuseness a_v, a_w in the volume central potential and corresponding parameters r_D, a_D in the surface central potential are considered [56]. To optimize global parameterization of alpha optical model potential [8], we performed χ^2 minimization of the cross sections for (n, α) reaction on ^{54}Fe using MINUIT package [50] and available experimental data mentioned above. In this way, we obtained the rescaling factors for the geometrical parameters of the global optical model potential from Ref. [8], as given in Table 1.

Table 1: Rescaling factors for the geometrical parameters in global alpha optical model potential [8] for ^{54}Fe and ^{118}Sn .

	^{54}Fe	^{118}Sn
r_v	0.94658	0.95283
a_v	1.05843	0.71722
r_w	0.80276	1.20286
a_w	1.19983	0.70011
r_D	1.01336	1.04916
a_D	1.09999	1.05427

The χ^2 values using adjusted optical model potential parameters (TALYS-1.96(a)) are shown in Table 2 in comparison to those of default TALYS-1.96 calculation and the corresponding χ^2 values obtained for a selection of other theoretical approaches, tabulated in JEFF-3.3 [78], ENDF/B-VII.1 [18], TENDL-2019 [60], BROND-3.1 [15], CENDL-3.2 [29], JENDL-5 [49], ROSFOND-2010 [4] and NON-SMOKER [85] data sets. The rescaling of the global optical model parameters provides improvement for the description of the (n, α) cross sections and in this way we benchmark the theory framework for further study of the Fe isotope chain.

Table 2: The χ^2 values for (n, α) cross sections for ^{54}Fe and ^{118}Sn in the present TALYS-1.96 calculation, in comparison to those calculated with the cross sections from other calculations. TALYS-1.96(a) denotes optimized calculation after adjustment of optical model parameters (see text for details).

	$\chi^2 ({}^{54}\text{Fe})$	$\chi^2 ({}^{118}\text{Sn})$
TALYS-1.96	3.14	27.606
TALYS-1.96(a)	2.61	11.65
JEFF-3.3 [78]	7.03	79.84
ENDF/B-VII.1 [18]	2.74	12.47
TENDL-2019 [60]	1.46	156.18
BROND-3.1 [15]	3.18	12.47
CENDL-3.2 [29]	2.86	75.14
JENDL-5 [49]	2.06	81.10
ROSFOND-2010 [4]	7.09	12.41
NON-SMOKER [85]	19.83	6426.48

The results of the present calculation of (n, α) reaction cross sections for ^{54}Fe are shown in Fig. 1 and Fig. 2 over the complete energy range up to 30 MeV. The cross

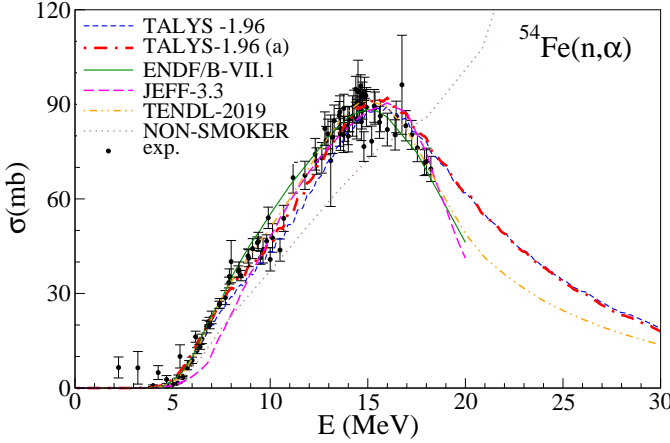


Figure 1: The (n, α) reaction cross section for ^{54}Fe from the present TALYS calculation in comparison with the experimental data [76, 68, 69, 67, 94, 37, 42, 88, 87, 54, 20, 66, 48] and various model calculations for ENDF/B-VII.1 [18], JEFF-3.3 [78], TENDL-2019 [60] and reaction code NON-SMOKER [92]. TALYS-1.96(a) denotes optimized calculation after adjustment of optical model parameters.

sections are compared with the collection of experimental data from various studies [76, 68, 69, 67, 94, 37, 42, 88, 87, 54, 20, 66, 48], as well as those of other calculations. We have restricted the comparison to the results summarized in Refs. ENDF/B-VII.1 [18], JEFF-3.3 [78], TENDL-2019 [60], NON-SMOKER [85], BROND-3.1 [15], JENDL-5 [49], CENDL-3.2 [29], and ROSFOND-2010 [4]. The results of the present model calculation, displaying the Gaussian-like shape of the cross sections characteristic for the compound nucleus reactions with particle emission, are in excellent agreement with the experimental data, that is improved in comparison to the previous studies. The maximal value of the cross section is obtained at neutron energy $E = 15.62$ MeV, that is very close to the peak energy from the experimental data as shown in Fig. 1 and Fig. 2. Although we do not consider low-energy cross sections in detail, we note that the largest sensitivity of the statistical model calculation of (n, α) cross sections corresponds to the lowest incident energies, where the level-density effects are not present [61]. For example, the cross sections in the present TALYS-1.96 and TALYS-1.96(a) calculations at energies below 4 MeV differ up to several orders of magnitude.

We employ the theory framework benchmarked on the experimental data for ^{54}Fe in the study of the evolution of the (n, α) reaction cross sections for Fe isotope chain. The results for the cross sections are shown in Fig. 3 for even-even isotopes $^{48-58}\text{Fe}$ (top panel) and even-odd isotopes $^{49-59}\text{Fe}$ (lower panel). For comparison, the experimental cross sections are also shown for a few additional isotopes with experimental data available, ^{56}Fe [9, 94, 88, 38, 55, 40, 25, 91], ^{57}Fe [54, 33], and ^{58}Fe [2, 19]. Excellent agreement of the calculated cross sections with experimental data for $^{56,57,58}\text{Fe}$ is obtained, without any additional adjustments. Thus, the established model set-

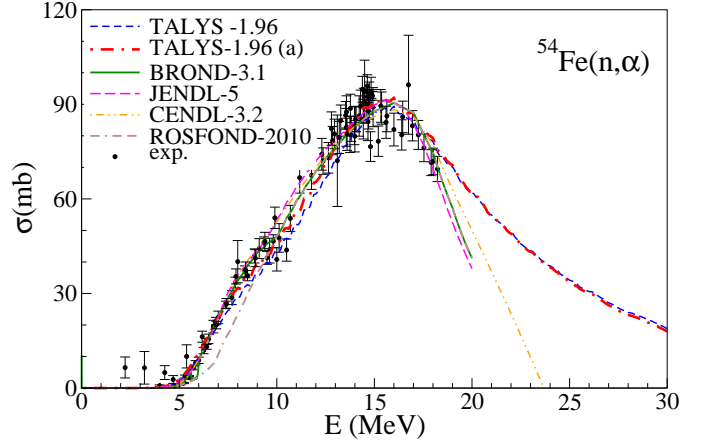


Figure 2: The same as Fig. 1 but BROND3.1 [15], JENDL-5 [29] and ROSFOND [84] model calculations are shown for comparison.

tings seem to be appropriate to study the systematics of the cross sections along the Fe isotope chain. For even-even Fe isotopes, with further increase of the neutron number, the cross sections become smaller. Similar behaviour can be observed for even-odd Fe isotopes. In order to understand this dependence of the cross sections, it is interesting to inspect the corresponding reaction Q -values along the isotope chain, as shown in Fig. 4. The Q -values systematically decrease with the number of neutrons, showing also odd-even staggering, thus, for more neutron rich isotopes more energy is required for the reaction. Emission of the α particle from the compound nucleus is determined by the probability for its formation within nucleus, and transmission probability for tunneling through the Coulomb barrier. The reaction cross section depends on the compound nucleus Coulomb barrier, since it suppresses the emission of outgoing ^4He . Although the height of the Coulomb barrier does not change along the isotope chain, it becomes spatially extended toward larger values of radial coordinate [63]. Finally, with increasing the neutron number, other particle emission channels also become more active, thus the α emission becomes reduced. We will discuss this aspect in more details.

Next we analyze the properties of the main peak of the cross section. Figure 5 shows the maximal value of the cross section and the corresponding neutron energy. The maximum of the cross section along the Fe isotope chain displays behaviour previously discussed, after reaching the largest value for ^{53}Fe , it is rapidly decreasing by almost two orders of magnitude for ^{59}Fe . The energy of the reaction cross section peak for $N > Z$ isotopes converges around ≈ 15 MeV. This saturation of the neutron energy required for the maximal (n, α) reaction cross section in isotopes with neutron excess appears as interesting feature of this reaction. The decrease of the cross section from its maximal value is in agreement with the isotope effect originally postulated in Ref.[28, 97] and confirmed in Ref.[73] on the basis of Q -values and the stable-isotope data. Rather

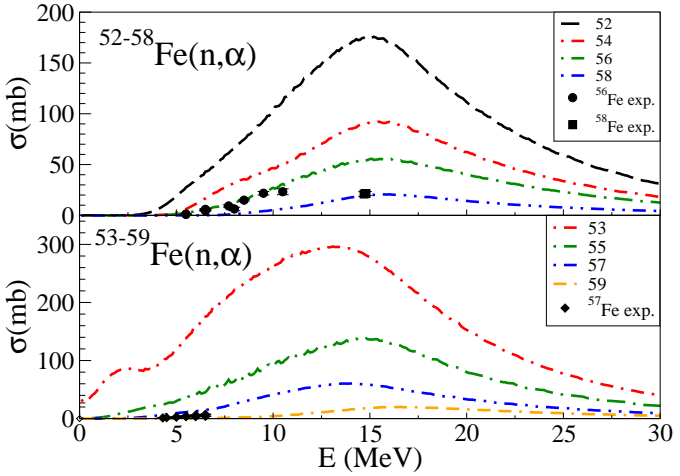


Figure 3: The (n, α) reaction cross sections for even-even isotopes $^{48-58}\text{Fe}$ (top panel) and even-odd isotopes $^{49-59}\text{Fe}$ (lower panel), based on TALYS-a calculation. The experimental cross sections are also shown for ^{56}Fe [9, 94, 88, 38, 55, 40, 25, 91], ^{57}Fe [54, 33], and ^{58}Fe [2, 19].

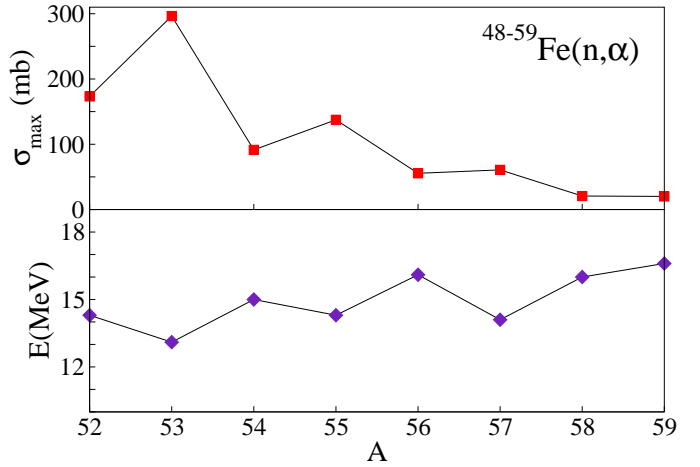


Figure 5: The maximal cross section value for (n, α) reaction for $^{46-67}\text{Fe}$ (upper panel) and the corresponding energy of the maximal cross section (lower panel).

constant energy around 15 MeV of the excitation-function maxima for stable isotopes also explains the former establishment of the isotope effect at this energy.

As mentioned before, one of the reasons for reducing the (n, α) reaction cross sections along the isotope chain are increasing contributions from other exit channels. For this purpose, in Fig. 6 the cross sections are shown for the neutron induced reactions with Fe isotopes for 5, 10, 15 and 20 MeV neutron energies and various exit channels, including γ , n , p , and α emission from the compound nucleus. For $^{46-53}\text{Fe}$ at all neutron energies the cross sections moderately increase, except for protons, showing odd-even staggering due to sensitivity on the pairing correlations. In the same mass region the cross section for the proton emission decreases, while the one for neutron emission increases, as expected for the increase of the neutron number in target nucleus. Of course, compound nucleus with excess of neutrons will favor emission of neutrons rather than protons, besides, neutrons are not affected by the Coulomb barrier. One can also observe an overall increase of the cross section for the gamma emission in the exit channel. Beyond ^{53}Fe the cross sections for α , as well as proton emission from the compound nucleus rapidly decrease, i.e. the corresponding cross sections reduce by several order of magnitude when compared to other shown exit channels. Clearly, for neutron rich Fe isotopes the (n, α) reaction cross section becomes negligible.

3.2. Sn isotopes

We extend our analysis of the (n, α) reaction cross sections to medium heavy mass region, for Sn isotopes as target nuclei. The cross section experimental data are rather limited and available over broader, though restricted, range of energies only for ^{118}Sn [83, 1, 14, 36, 62, 13, 5, 65]. Similar as for Fe isotopes, first we adjust the settings of the model by using experimental data for ^{118}Sn . We constrain the parameters of the alpha global optical model potential,

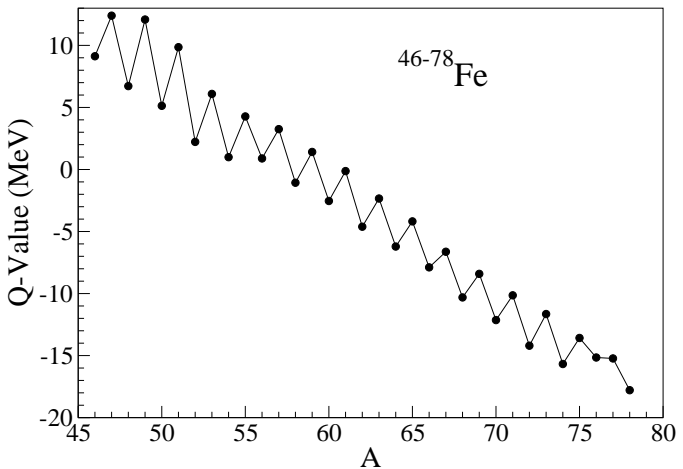


Figure 4: The (n, α) reaction Q -value for Fe isotopes.

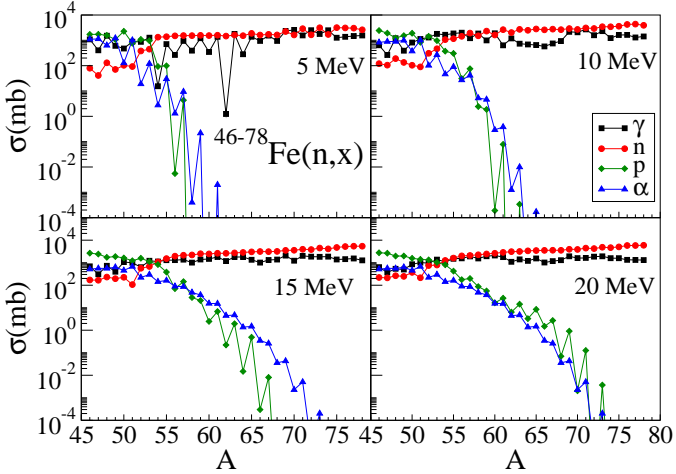


Figure 6: The cross sections for neutron induced reactions with $^{46-78}\text{Fe}$ target for gamma, neutron, proton and alpha emission from the compound nucleus, shown at 5, 10, 15 and 20 MeV neutron energies.

r_v , a_v , r_w , a_w , r_D , a_D , by χ^2 minimization of the (n, α) cross sections for ^{118}Sn using the experimental data from Refs. [83, 1, 14, 36, 62, 13, 5, 65]. The resulting rescaling factors of the global optical model potential from Ref. [8] are shown in Table 1. Furthermore, Table 2 shows the χ^2 value obtained by adjusting the optical model parameters in the present TALYS calculation, in comparison to the corresponding χ^2 values obtained from other calculations [78, 85, 18, 60, 15, 29, 49, 4]. The present adjustment of the optical model results in improved description of the (n, α) cross sections, and in this way we benchmark the model for systematic studies of the cross sections along Sn isotope chain.

The resulting (n, α) cross sections for ^{118}Sn are shown in Fig. 7 and Fig. 8, in comparison to experimental data [83, 1, 14, 36, 62, 13, 5, 65] and calculations from Refs. [78, 18, 49, 29, 60, 15, 4, 16, 49, 85]. Due to limited data, from the experimental side it is not possible to observe the complete shape of the cross section, while the present TALYS calculation results in a Gaussian-like shape of the cross section peaked around 22.27 MeV. In comparison to other studies, that often have restricted energy range for the cross sections, the present calculation represents considerable improvement, especially when compared to NON-SMOKER [85] and TENDL-2019 [60]. However, for a complete understanding of the (n, α) cross sections, more experimental data are required, covering a broader range of neutron energies, as shown in Fig. 7 and Fig. 8.

By using TALYS calculation with previously established rescaling for the optical model parameters, in Fig. 9 the (n, α) cross sections are shown for the range of isotopes $^{102-116}\text{Sn}$, separately for even-even and even-odd nuclei. In the former case, the overall cross sections reach their maximal values for ^{106}Sn , and they further systematically decrease till ^{116}Sn , resulting with very small values, e.g. its maximal cross section at $E = 20.68$ MeV is only

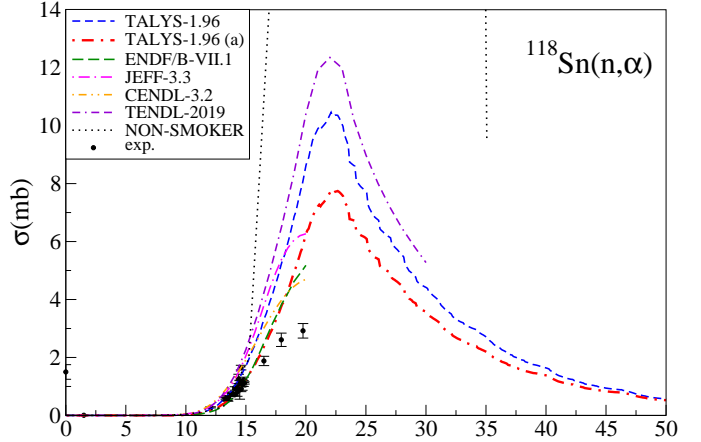


Figure 7: The (n, α) reaction cross sections for ^{118}Sn . The present TALYS-a calculation is compared with experimental data [83, 1, 14, 36, 62, 13, 5, 65] and other theoretical approaches [78, 18, 29, 60, 85].

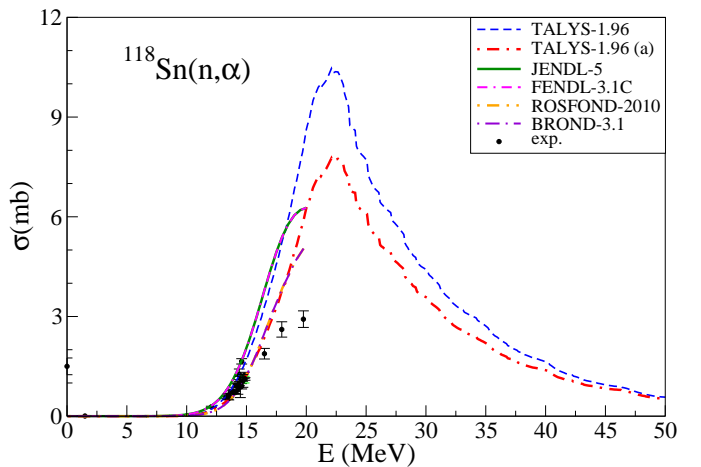


Figure 8: The (n, α) reaction cross sections for ^{118}Sn . The present TALYS-a calculation is compared with experimental data [83, 1, 14, 36, 62, 13, 5, 65] and other theoretical approaches. [49, 15, 4, 49, 16].

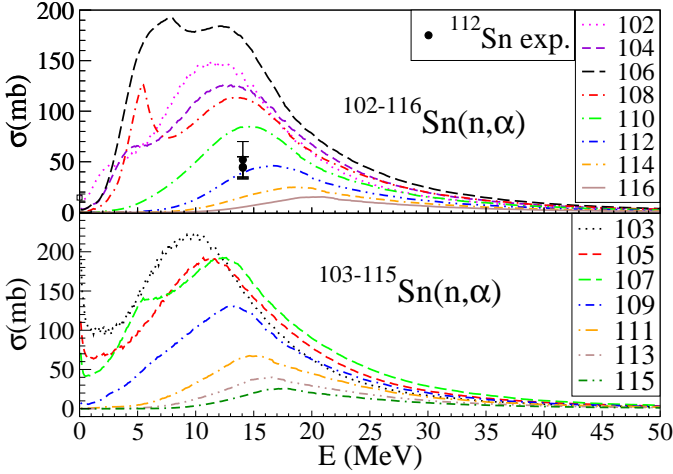


Figure 9: The (n, α) reaction cross sections for $^{102-116}\text{Sn}$, shown

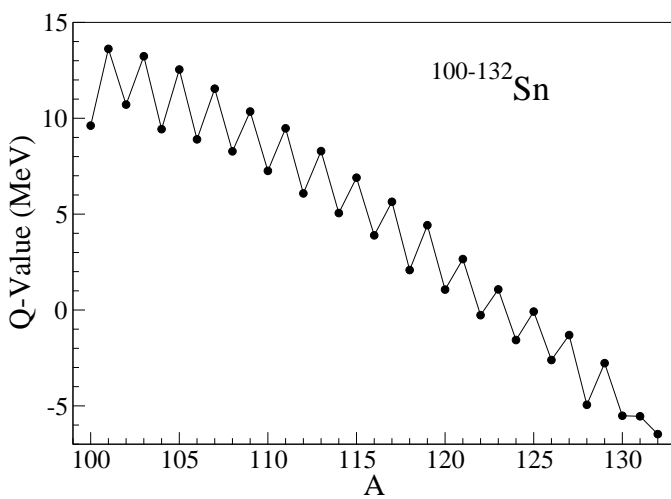


Figure 10: The (n, α) reaction Q -value for Sn isotopes.

16.01 mb, in comparison to ^{106}Sn at $E = 7.8$ MeV, where $\sigma = 194.17\text{mb}$. As shown in the lower panel of Fig. 9, similar behaviour of the cross sections is also obtained for even-odd Sn isotopes, with the maximal cross section obtained for ^{103}Sn . Qualitatively, with increasing the neutron number, we obtain similar behaviour of the (n, α) cross sections as previously shown for Fe isotopes, and the same discussion on their isotopic dependence also applies for Sn isotopes. The dependence of the cross sections is also determined by the reaction Q -value, which systematically decreases along the Sn isotope chain, with odd-even staggering, as shown in Fig. 10.

To analyse the systematic behaviour of the (n, α) cross sections for Sn isotopes, in Fig. 11 the maximal values or the cross sections and the corresponding neutron energies are shown for $^{102-116}\text{Sn}$. The maximal cross section peaks are obtained for ^{106}Sn (even-even isotopes) and ^{103}Sn (even-odd isotopes). With further increase of the neutron number, more energy of the incoming neutrons is

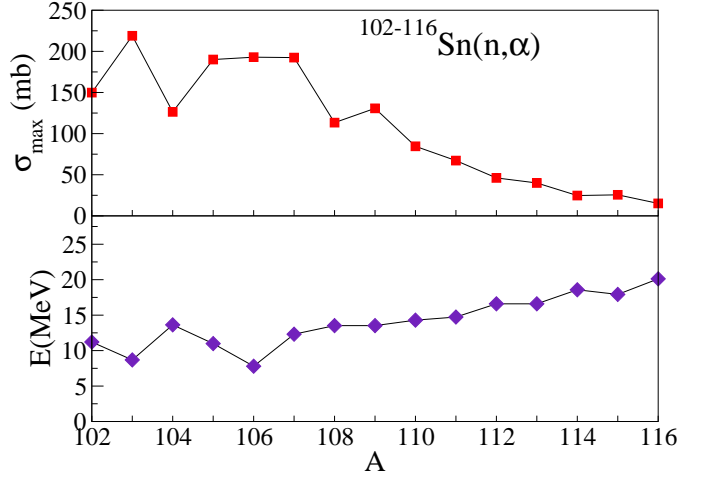


Figure 11: Evolution of the cross sections and neutron energy for the $^{102-116}\text{Sn}(n, \alpha)$ reaction.

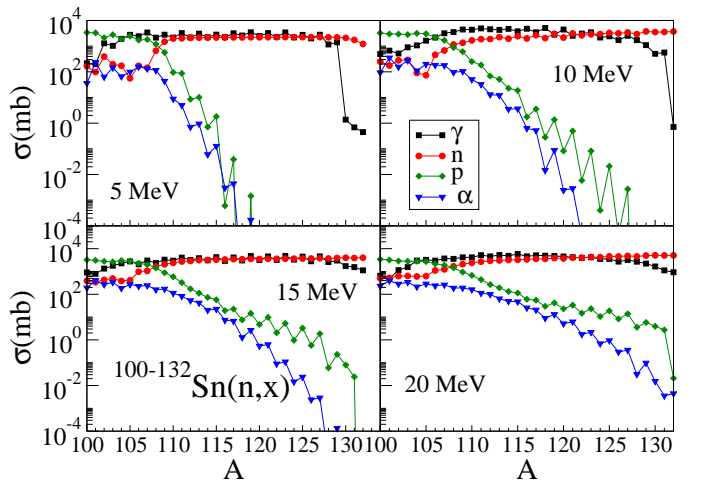


Figure 12: The same as Fig. 6, but for $^{100-132}\text{Sn}$ isotopes.

required for the reaction, in agreement with the evolution of the Q -value with the neutron number, as shown in Fig. 10. Lower panel of Fig. 11 also shows the saturation of the neutron energy of the maximal cross section with increase of the neutron number, though slight increase of the cross section with the energy is obtained.

Figure 12 shows the evolution of the cross sections for neutron induced reactions for $^{100-132}\text{Sn}$ at neutron energies 5, 10, 15, and 20 MeV, by considering γ , n , p , and α exit channels. In general, the cross sections for p and α emission systematically reduce with the neutron number, while those for the neutron and gamma emission increase or saturate, as expected for compound nuclei with larger number of neutrons. Some deviations are obtained for gamma emission involving nuclei with large neutron excess. The reduction of (n, γ) cross sections for $^{129-132}\text{Sn}$ for neutron energies of 5 and 10 MeV appears due to the overall shift of the cross sections toward higher energies, similar as observed in Fig. 9 for (n, α) reaction.

3.3. Maxwellian averaged cross sections along Fe and Sn isotope chains

Since (n, α) reactions also contribute to the nucleosynthesis, it is interesting to explore the isotopic dependence of the cross sections in stellar environment. Only small modifications of the neutron capture reaction cross sections could have important implications on the path of nuclear processes contributing to the synthesis of chemical elements [21]. We investigate the Maxwellian averaged cross sections (MACS), that take into account Maxwell-Boltzmann distribution for neutrons with respect to the corresponding temperature [82]. In the present study, two temperatures characteristic for stellar environment are considered, $kT = 30$ keV (e.g., associated to the core He burning in massive stars), and $kT = 90$ keV (e.g., in supernova envelope where the r-process could occur) [77, 51, 6].

So far, available information on the MACS values for (n, α) reactions with Fe and Sn isotopes is rather limited. At 30 keV, for $^{46-78}\text{Fe}$ isotopes the only calculations are available for ^{55}Fe [98], ^{57}Fe [81] and ^{59}Fe [98]. For $^{100-132}\text{Sn}$ isotopes at 30 keV, there are also only a few available MACS values. For $^{112,113,115,117}\text{Sn}$, there are a few calculations [17, 18, 81, 90, 98, 89, 30], but for ^{121}Sn [98] and $^{114,119,123,125,126}\text{Sn}$ [89, 81] there are results only from one calculation. At 90 keV, there are MACS values for $^{54,55,56,57,59}\text{Fe}$ in Refs. [90, 89, 30, 98, 17, 18, 81]. For $^{112,113,114,115,117}\text{Sn}$ a few results exist in Refs. [17, 18, 81, 90, 89, 4, 30]. For $^{119,121,123,125}\text{Sn}$ there exists only one result for each isotope [89, 98, 81]. Thus we perform a systematic calculation of the MACS values over Fe and Sn isotope chains. For comparison, in addition to the (n, α) reaction, also other exit channels from the neutron induced reactions are studied.

Figure 13 shows the Maxwellian averaged cross sections for $^{46-78}\text{Fe}$ isotopes with temperature corresponding to $kT = 30$ keV (top panel) and $kT = 90$ keV (lower panel), for the neutron induced reactions with γ , n , p , and α emission from compound nucleus. For $kT = 30$ keV, for lighter Fe isotopes one can observe that α emission has large contributions comparable as those with γ , n and p emission. Especially for $^{46,47,48,49,51}\text{Fe}$, the cross section for α exit channel is the most dominant, and for $^{50,53,55}\text{Fe}$ it also has relevant contribution. As expected from the previous analysis of the cross sections, the MACS values also rapidly decrease for the neutron-rich isotopes. One can also observe the sensitivity of the results on temperature, resulting in the reduction of the MACS values and modifications in their evolution along the isotope chains.

Similar analysis of the MACS values is also performed for $^{100-126}\text{Sn}$ at $kT = 30$ keV and $kT = 90$ keV. In Fig. 14 the corresponding MACS results are shown separately for γ , n , p , and α emission in the exit channels. While the MACS values for α emission are decreasing and becoming negligible for target nuclei with larger number of neutrons, for isotopes $^{100-107}\text{Sn}$ the α emission also contributes, though not as dominant channel. Further more

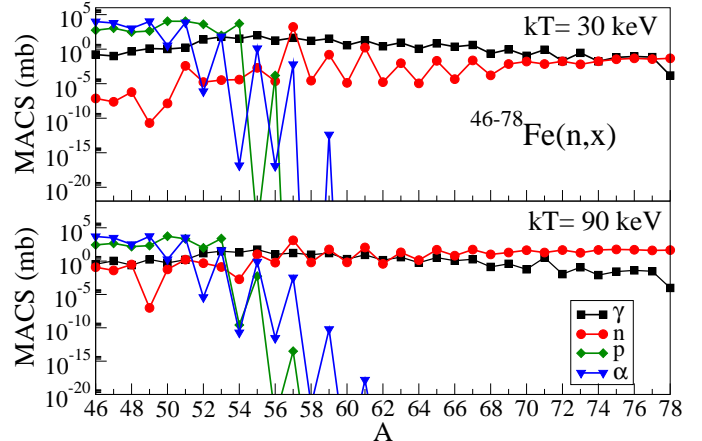


Figure 13: The Maxwellian averaged cross sections (MACS) for neu-

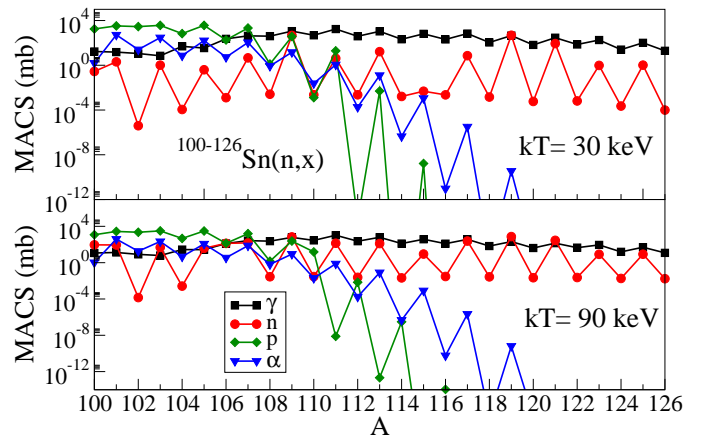


Figure 14: The same as Fig.13, but for $^{100-126}\text{Sn}$.

systematic studies, along the nuclide map, are required to explore in more details the contributions of nuclei with considerable (n, α) reaction cross sections to the nucleosynthesis.

4. Conclusion

In this work we have investigated the evolution of (n, α) reaction cross sections for target nuclei within Fe and Sn isotope chains. Model calculations have been performed in the theory framework based on Hauser-Feshbach statistical model and exciton model through their implementation in the nuclear reaction code TALYS [59], using Skyrme functional to describe nuclear masses and back-shifted Fermi gas model level densities. Global optical model potential has been used, with additionally adjusted rescaling of the mass dependent geometrical parameters, obtained by χ^2 minimization using experimental data for ^{54}Fe and ^{118}Sn to benchmark the model for studies of (n, α) reactions along the respective isotope chains. In this way, the present model calculations resulted in considerable improvement compared to previous studies. It remains open

question how reliable are adjusted optical model potentials for isotopes away from ^{54}Fe and ^{118}Sn used to improve the description of (n, α) reaction cross sections. The available data on $^{56,58}\text{Fe}$ and ^{112}Sn are well reproduced, however, more experimental studies on (n, α) reaction cross sections are required to assess the quality of the optical model potentials when extrapolating to neutron-rich isotopes.

Since the experimental data on (n, α) reaction cross sections are rather limited for Fe and Sn isotopes, and often restricted to narrow energy range, model calculations in this work provide insight how the cross sections vary with increasing neutron number, by considering complete relevant neutron energy range. It is shown that (n, α) reaction cross section have larger values for lighter isotopes for both isotope chains, and their maximal values are obtained for ^{53}Fe and ^{103}Sn , respectively. By further increasing the neutron number in target nucleus, the (n, α) reaction cross section becomes smaller due to decreasing of the reaction Q -value and opening other more dominant exit channels, as shown in the analysis that in addition to α emission included also neutron, proton, and γ emission. The neutron energy has an effective role for the (n, α) cross section, i.e., neutrons with higher energies can induce reactions in heavier isotopes. The analysis of Maxwellian averaged cross sections showed dominant or considerable contributions of (n, α) reactions over other exit channels for lower mass Fe isotopes. Throughout the isotope chains, while going to neutron-rich isotopes, cross section values strongly decrease. Thus, the (n, α) reactions are not effective for very neutron rich nuclei, and their role in the nucleosynthesis that goes through the neutron-rich side of the nuclide map, such as the r-process, is negligible. While the (n, α) reactions dominate for low-mass Fe isotopes, in nuclei with neutron excess γ and neutron emission are dominating outcomes from neutron induced reactions, with varying contributions dependent on temperature involved. Further studies are required to assess the role of (n, α) reactions in nucleosynthesis, in cases of nuclei with significant respective cross sections.

5. Acknowledgements

This work is supported by the QuantiXLie Centre of Excellence, a project co-financed by the Croatian Government and European Union through the European Regional Development Fund, the Competitiveness and Cohesion Operational Programme (KK.01.1.1.01.0004). S.K. acknowledges support from the Scientific and Technological Research Council of Turkey (TUBITAK) through the International Doctoral Research Fellowship Programme 2214A, 2020/1, Grant No. 1059B142000254.

References

- [1] A.A.Filatenkov, 2016. Neutron activation cross sections measured at kri in neutron energy region 13.4 - 14.9 mev. International Atomic Energy Agency INDC(CCP)-0460, 1-277. URL: <https://www-nds.iaea.org/publications/indc/indc-ccp-0460/>.
- [2] A.D.Majdeddin, V.Semkova, R.Doczi, Cs.M.Buczko, J.Csikai, 1997. Investigations on (n, α) cross sections in the 14 mev region. International Atomic Energy Agency 28, 20.
- [3] Al-Khasawneh, K., Borris, E., Bruückner, B., Eberhardt, K., Erbacher, P., Fiebiger, S., Germhäuser, R., Göobel, K., Heftrich, T., Kisselbach, T., Kurtulgil, D., Langer, C., Reich, M., Reifarth, R., Renisch, D., Thomas, B., Volknandt, M., Weigand, M., 2020. Nice - neutron induced charged particle emission. Journal of Physics: Conference Series 1668, 012021. URL: <http://dx.doi.org/10.1088/1742-6596/1668/1/012021>, doi:[10.1088/1742-6596/1668/1/012021](https://doi.org/10.1088/1742-6596/1668/1/012021).
- [4] Andrianova, O.N., Golovko, Y.Y., Manturov, G.N., 2019. Verification of the rosfond/abbn nuclear data based on the oecd/nea benchmark on criticality safety of mox-fueled systems. Nuclear Energy and Technology 5, 91–96. URL: <https://doi.org/10.3897/nucet.5.35577>, doi:[10.3897/nucet.5.35577](https://doi.org/10.3897/nucet.5.35577).
- [5] Arif, M., Zaidi, J., Qureshi, I., Nilore, P., Iqbal, M.Z., 1996. Fission neutron spectrum averaged cross sections of some threshold reactions on tin: Small scale production of ^{111}In in a nuclear reactor. Radiochimica Acta 75, 175–178.
- [6] Arnould, M., Goriely, S., Takahashi, K., 2007. The r-process of stellar nucleosynthesis: Astrophysics and nuclear physics achievements and mysteries. Physics Reports 450, 97–213. URL: <https://www.sciencedirect.com/science/article/pii/S0370157307002202>, doi:<https://doi.org/10.1016/j.physrep.2007.06.002>.
- [7] Avrigeanu, M., von Oertzen, W., Plompen, A., Avrigeanu, V., 2003. Optical model potentials for α -particles scattering around the coulomb barrier on a 100 nuclei. Nuclear Physics A 723, 104–126. URL: <https://www.sciencedirect.com/science/article/pii/S0375947403011159>, doi:[https://doi.org/10.1016/S0375-9474\(03\)01159-X](https://doi.org/10.1016/S0375-9474(03)01159-X).
- [8] Avrigeanu, V., Avrigeanu, M., Măñăilescu, C., 2014. Further explorations of the α -particle optical model potential at low energies for the mass range $a \approx 45$ –209. Phys. Rev. C 90, 044612. URL: <https://link.aps.org/doi/10.1103/PhysRevC.90.044612>, doi:[10.1103/PhysRevC.90.044612](https://doi.org/10.1103/PhysRevC.90.044612).
- [9] Bai, H., Jiang, H., Lu, Y., Cui, Z., Chen, J., Zhang, G., Glendenov, Y.M., Sedysheva, M.V., Khuukhenkhuu, G., Ruan, X., Huang, H., Ren, J., Fan, Q., 2019. $^{56,54}\text{Fe}(n, \alpha)^{53,51}\text{Cr}$ cross sections in the mev region. Phys. Rev. C 99, 024619. URL: <https://link.aps.org/doi/10.1103/PhysRevC.99.024619>, doi:[10.1103/PhysRevC.99.024619](https://doi.org/10.1103/PhysRevC.99.024619).
- [10] Banerjee, P., Heger, A., Qian, Y.Z., 2019. New s-process mechanism in rapidly rotating massive population II stars. The Astrophysical Journal 887, 187. URL: <https://doi.org/10.3847/1538-4357/ab517a>, doi:[10.3847/1538-4357/ab517a](https://doi.org/10.3847/1538-4357/ab517a).
- [11] Barbagallo, M., Musumarra, A., Cosentino, L., Maugeri, E., Heinitz, S., Mengoni, A., Dressler, R., Schumann, D., Käppeler, F., Colonna, N., Finocchiaro, P., Ayranov, M., Damone, L., Kivel, N., Aberle, O., Altstadt, S., Andrzejewski, J., Audouin, L., Bacak, M., Balibrea-Correa, J., Barros, S., Bécares, V., Bečvář, F., Beinrucker, C., Berthoumieux, E., Billowes, J., Bosnar, D., Brugger, M., Caamaño, M., Calviani, M., Calviño, F., Cano-Ott, D., Cardella, R., Casanovas, A., Castelluccio, D.M., Cerutti, F., Chen, Y.H., Chiaveri, E., Cortés, G., Cortés-Giraldo, M.A., Cristallo, S., Diakaki, M., Domingo-Pardo, C., Dupont, E., Duran, I., Fernandez-Dominguez, B., Ferrari, A., Ferreira, P., Furman, W., Ganesan, S., García-Rios, A., Gawlik, A., Glodariu, T., Göbel, K., Gonçalves, I.F., González-Romero, E., Griesmayer, E., Guerrero, C., Gunsing, F., Harada, H., Heftrich, T., Heyse, J., Jenkins, D.G., Jericha, E., Katauchi, T., Kavrigin, P., Kimura, A., Kokkoris, M., Krtička, M., Leal-Cidoncha, E., Lerendegui, J., Lederer, C., Leeb, H., Lo Meo, S., Lonsdale, S.J., Losito, R., Macina, D., Marganiec, J., Martínez, T., Massimi, C., Mastinu, P., Mastromarco, M., Mazzone, A., Mendoza, E., Milazzo, P.M., Mingrone, F., Mirea, M., Montesano, S., Nolte, R., Oprea, A., Pappalardo, A., Patronis, N., Pavlik, A., Perkowski, J.,

- Piscopo, M., Plompen, A., Porras, I., Praena, J., Quesada, J., Rajeev, K., Rauscher, T., Reifarth, R., Riego-Perez, A., Rout, P., Rubbia, C., Ryan, J., Sabate-Gilarte, M., Saxena, A., Schillebeeckx, P., Schmidt, S., Sedyshev, P., Smith, A.G., Stamatopoulos, A., Tagliente, G., Tain, J.L., Tarifeño Saldívia, A., Tassan-Got, L., Tsinganis, A., Valenta, S., Vannini, G., Variale, V., Vaz, P., Ventura, A., Vlachoudis, V., Vlastou, R., Vollaire, J., Wallner, A., Warren, S., Weigand, M., Weiß, C., Wolf, C., Woods, P.J., Wright, T., Žugec, P. (n -TOF Collaboration), 2016. $^7\text{Be}(n, \alpha)^4\text{He}$ reaction and the cosmological lithium problem: Measurement of the cross section in a wide energy range at n_{tof} at cern. Phys. Rev. Lett. 117, 152701. URL: <https://link.aps.org/doi/10.1103/PhysRevLett.117.152701>, doi:[10.1103/PhysRevLett.117.152701](https://doi.org/10.1103/PhysRevLett.117.152701).
- [12] Barth, R.F., Coderre, J.A., Vicente, M.G.H., Blue, T.E., 2005. Boron neutron capture therapy of cancer: Current status and future prospects. Clinical Cancer Research 11, 3987–4002. URL: <https://clincancerres.aacrjournals.org/content/11/11/3987>, doi:[10.1158/1078-0432.CCR-05-0035](https://doi.org/10.1158/1078-0432.CCR-05-0035).
- [13] Bayhurst, B., Prestwood, R., 1961. (n, p) and (n, α) excitation functions of several nuclei from 7- 0 to 19- 8 mev. Journal of Inorganic and Nuclear Chemistry 23, 173–185.
- [14] Beták, E., Mikolajczak, R., Staniszewska, J., Mikolajewski, S., Rurarz, E., 2005. Activation cross sections for reactions induced by 14 mev neutrons on natural tin and enriched ^{112}Sn targets with reference to ^{111}In production via radioisotope generator $^{112}\text{Sn}(n, 2n)^{111}\text{Sn} \rightarrow ^{111}\text{In}$. Radiochimica Acta 93, 311–326. URL: <https://doi.org/10.1524/ract.93.6.311.65644>, doi:[10.1524/ract.93.6.311.65644](https://doi.org/10.1524/ract.93.6.311.65644).
- [15] Blokhin, A.I., Gai, E.V., Ignatyuk, A.V., Koba, I.I., Manokhin, V.N., Pronyaev, V.N., 2016. New version of neutron evaluated data library brond-3.1. Yad. Reak. Konst. 2, 62.
- [16] Capote, R., Otsuka, N., Kawano, T., Koning, A., Kuñieda, S., Sublet, J.C., Watanabe, Y., 2012. Fendl-3 library—summary documentation. International Atomic Energy Agency INDC (NDS)-628, 1–26. URL: <https://www-nds.iaea.org/publications/indc/indc-nds-0628/>.
- [17] Chadwick, M., Obložinský, P., Herman, M., Greene, N., McKnight, R., Smith, D., Young, P., MacFarlane, R., Hale, G., Frankle, S., Kahler, A., Kawano, T., Little, R., Madland, D., Moller, P., Mosteller, R., Page, P., Talou, P., Trellue, H., White, M., Wilson, W., Arcilla, R., Dunford, C., Mughabghab, S., Pritychenko, B., Rochman, D., Sonzogni, A., Lubitz, C., Trumbull, T., Weinman, J., Brown, D., Cullen, D., Heinrichs, D., McNabb, D., Derrien, H., Dunn, M., Larson, N., Leal, L., Carlson, A., Block, R., Briggs, J., Cheng, E., Huria, H., Zerkle, M., Kozier, K., Courcelle, A., Pronyaev, V., van der Marck, S., 2006. Endf/b-vii.0: Next generation evaluated nuclear data library for nuclear science and technology. Nuclear Data Sheets 107, 2931–3060. URL: <https://www.sciencedirect.com/science/article/pii/S0090375206000870>, doi:<https://doi.org/10.1016/j.nds.2006.11.001>.
- [18] Chadwick, M.B., Herman, M., Obložinský, P., Dunn, M.E., Danon, Y., Kahler, A.C., Smith, D.L., Pritychenko, B., Arbanas, G., Arcilla, R., Brewer, R., Brown, D.A., Capote, R., Carlson, A.D., Cho, Y.S., Derrien, H., Guber, K., Hale, G.M., Hoblit, S., Holloway, S., Johnson, T.D., Kawano, T., Kiedrowski, B.C., Kim, H., Kunieda, S., Larson, N.M., Leal, L., Lestone, J.P., Little, R.C., McCutchan, E.A., MacFarlane, R.E., MacInnes, M., Mattoon, C.M., McKnight, R.D., Mughabghab, S.F., Nobre, G.P.A., Palmiotti, G., Palumbo, A., Pigni, M.T., Pronyaev, V.G., Sayer, R.O., Sonzogni, A.A., Summers, N.C., Talou, P., Thompson, I.J., Trkov, A., Vogt, R.L., van der Marck, S.C., Wallner, A., White, M.C., Wiarda, D., Young, P.G., 2011. Nuclear Data Sheets 112, 2887–2996.
- [19] Chittenden, D.M., Gardner, D.G., Fink, R.W., 1961. New isotope of manganese; cross sections of the iron isotopes for 14.8-mev neutrons. Phys. Rev. 122, 860–861. URL: <https://link.aps.org/doi/10.1103/PhysRev.122.860>, doi:[10.1103/PhysRev.122.860](https://doi.org/10.1103/PhysRev.122.860).
- [20] Cross, W.G., Clarke, R.L., Morin, K., Slinn, G., Ahmed, N.M., Beg, K., 1963. Activation cross sections of fe and ni isotopes for 14.5 mev neutrons. Canadian report to EANDC , 1.
- [21] Dan, M., Singh, G., Chatterjee, R., Shubhchintak, 2019. Neutron capture rates of ^{18}C . Phys. Rev. C 99, 035801. URL: <https://link.aps.org/doi/10.1103/PhysRevC.99.035801>, doi:[10.1103/PhysRevC.99.035801](https://doi.org/10.1103/PhysRevC.99.035801).
- [22] De Smet, L., Wagemans, C., Goeminne, G., Heyse, J., Van Gils, J., 2007. Experimental determination of the $^{36}\text{Cl}(n, p)^{36}\text{S}$ and $^{36}\text{Cl}(n, \alpha)^{33}\text{P}$ reaction cross sections and the consequences on the origin of ^{36}S . Phys. Rev. C 75, 034617. URL: <https://link.aps.org/doi/10.1103/PhysRevC.75.034617>, doi:[10.1103/PhysRevC.75.034617](https://doi.org/10.1103/PhysRevC.75.034617).
- [23] Dilg, W., Schantl, W., Vonach, H., Uhl, M., 1973. Level density parameters for the back-shifted fermi gas model in the mass range $40 < a < 250$. Nuclear Physics A 217, 269–298.
- [24] Farwell, G.W., Wegner, H.E., 1954. Elastic scattering of intermediate-energy alpha particles by heavy nuclei. Phys. Rev. 95, 1212–1217. URL: <https://link.aps.org/doi/10.1103/PhysRev.95.1212>, doi:[10.1103/PhysRev.95.1212](https://doi.org/10.1103/PhysRev.95.1212).
- [25] Fischer, U.R., Traxler, G., Uhl, M., Vonach, H., 1984. Fe-56 (n, α) Cr-53 and Ni-60 (n, α) Fe-57 reactions at En=14.1 MeV. Phys. Rev. C 30, 72–78. doi:[10.1103/PhysRevC.30.72](https://doi.org/10.1103/PhysRevC.30.72).
- [26] Fotiades, N., Devlin, M., Haight, R.C., Nelson, R.O., Kunieda, S., Kawano, T., 2015. α and $2p2n$ emission in fast neutron-induced reactions on ^{60}Ni . Phys. Rev. C 91, 064614. URL: <https://link.aps.org/doi/10.1103/PhysRevC.91.064614>, doi:[10.1103/PhysRevC.91.064614](https://doi.org/10.1103/PhysRevC.91.064614).
- [27] Freiburghaus, C., Rosswog, S., Thielemann, F.K., 1999. r-process in neutron star mergers. The Astrophysical Journal 525, L121–L124. URL: <https://doi.org/10.1086/312343>, doi:[10.1086/312343](https://doi.org/10.1086/312343).
- [28] Gardner, D.G., Yu-Wen, Y., 1964. Trends in nuclear reaction cross sections (iii). the (n, α) reaction induced by 14.5 mev neutrons for elements in the range $6 < z < 30$. Nuclear Physics 60, 49–64. URL: <https://www.sciencedirect.com/science/article/pii/0029558264900007>, doi:[https://doi.org/10.1016/0029-5582\(64\)90005-7](https://doi.org/10.1016/0029-5582(64)90005-7).
- [29] Ge, Z., Xu, R., Wu, H., Zhang, Y., Chen, G., Jin, Y., Shu, N., Chen, Y., Tao, X., Tian, Y., Liu, P., Qian, J., Wang, J., Zhang, H., Liu, L., Huang, X., 2020. Cendl-3.2: The new version of chinese general purpose evaluated nuclear data library. EPJ Web Conf. 239, 09001. URL: <https://doi.org/10.1051/epjconf/202023909001>.
- [30] Ge, Z., Zhao, Z., Xia, H., Zhuang, Y., Liu, T., Zhang, J., Wu, H., 2011. The updated vversion of chinese evaluated nuclear data library (cendl-3.1). Journal of the Korean Physical Society 59, 1052–1056. doi:[10.3938/jkps.59.1052](https://doi.org/10.3938/jkps.59.1052).
- [31] Gledenov, Y.M., Koehler, P.E., Andrzejewski, J., Guber, K.H., Rauscher, T., 2000. $^{147}\text{Sm}(n, \alpha)$ cross section measurements from 3 ev to 500 kev: Implications for explosive nucleosynthesis reaction rates. Phys. Rev. C 62, 042801(R). URL: <https://link.aps.org/doi/10.1103/PhysRevC.62.042801>, doi:[10.1103/PhysRevC.62.042801](https://doi.org/10.1103/PhysRevC.62.042801).
- [32] Gledenov, Y.M., Sedysheva, M.V., Khuukhenkhuu, G., Bai, H., Jiang, H., Lu, Y., Cui, Z., Chen, J., Zhang, G., 2018. Measurement of the cross sections of the $^{25}\text{Mg}(n, \alpha)^{22}\text{Ne}$ reaction in the 4–6 mev region. Phys. Rev. C 98, 034605. URL: <https://link.aps.org/doi/10.1103/PhysRevC.98.034605>, doi:[10.1103/PhysRevC.98.034605](https://doi.org/10.1103/PhysRevC.98.034605).
- [33] Gledenov, Y.M., Sedysheva, M.V., Stolupin, V.A., Zhang, G., Han, J., Wang, Z., Fan, X., Liu, X., Chen, J., Khuukhenkhuu, G., Szalanski, P.J., 2014. Cross sections of the $^{57}\text{Fe}(n, \alpha)^{54}\text{Cr}$ and $^{63}\text{Cu}(n, \alpha)^{60}\text{Co}$ reactions in the mev region. Phys. Rev. C 89, 064607. URL: <https://link.aps.org/doi/10.1103/PhysRevC.89.064607>, doi:[10.1103/PhysRevC.89.064607](https://doi.org/10.1103/PhysRevC.89.064607).
- [34] Goeminne, G., Wagemans, C., Wagemans, J., Serot, O., Loiselet, M., Gaelens, M., 2000. Investigation of the $^{37}\text{Ar}(n, p)^{37}\text{Cl}$ and $^{37}\text{Ar}(n, \alpha)^{34}\text{S}$ reactions in the neutron energy range from 10 mev to 100 kev. Nuclear Physics A 678, 11–23. URL:

- <https://www.sciencedirect.com/science/article/pii/S037594740003122>
- [35] Goriely, S., Chamel, N., Pearson, J.M., 2009. Skyrme-hartree-fock-bogoliubov nuclear mass formulas: Crossing the 0.6 mev accuracy threshold with microscopically deduced pairing. Phys. Rev. Lett. 102, 152503. URL: <https://link.aps.org/doi/10.1103/PhysRevLett.102.152503>, doi:[10.1103/PhysRevLett.102.152503](https://doi.org/10.1103/PhysRevLett.102.152503).
- [36] Grallert, A., Csikai, J., Buczktf, C.M., Shaddad, I., 1993. Investigations on the systematics in (n, α) cross sections. International Atomic Energy Agency INDC(NDS)-286/L, 131. URL: <https://www-nds.iaea.org/publications/indc/indc-nds-0286/>.
- [37] Greenwood, L., 1987. in: Influence of Radiation on Mat. Proper, ASTM International.
- [38] Grimes, S.M., Haight, R.C., Alvar, K.R., Barschall, H.H., Borchers, R.R., 1979. Charged-particle emission in reactions of 15-mev neutrons with isotopes of chromium, iron, nickel, and copper. Phys. Rev. C 19, 2127–2137. URL: <https://link.aps.org/doi/10.1103/PhysRevC.19.2127>, doi:[10.1103/PhysRevC.19.2127](https://doi.org/10.1103/PhysRevC.19.2127).
- [39] Gyürky, G., Fülop, Z., Käppeler, F., Kiss, G.G., Wallner, A., 2019. The activation method for cross section measurements in nuclear astrophysics. The European Physical Journal A 55, 41. URL: <https://doi.org/10.1140/epja/i2019-12708-4>, doi:[10.1140/epja/i2019-12708-4](https://doi.org/10.1140/epja/i2019-12708-4).
- [40] Haight, R.C., Kneff, D.W., Oliver, B.M., Greenwood, L.R., Vonach, H., 1996. Helium production by 9.85-mev neutrons in elemental iron, nickel, and copper and in 56fe and 58,60,61ni. Nuclear Science and Engineering 124, 219–227. URL: <https://doi.org/10.13182/NSE96-A28573>, doi:[10.13182/NSE96-A28573](https://doi.org/10.13182/NSE96-A28573).
- [41] Hampel, M., Stancliffe, R.J., Lugaro, M., Meyer, B.S., 2016. THE INTERMEDIATE NEUTRON-CAPTURE PROCESS AND CARBON-ENHANCED METAL-POOR STARS. The Astrophysical Journal 831, 171. URL: <https://doi.org/10.3847/0004-637x/831/2/171>, doi:[10.3847/0004-637x/831/2/171](https://doi.org/10.3847/0004-637x/831/2/171).
- [42] Han-Lin, L., Ji-Zhou, L., Pei-Guo, F., Jian-Zhou, H., 1989. Compilation of measurements and evaluations of nuclear activation cross sections for nuclear data applications. International Atomic Energy Agency INDC(CPR)-16, 1–60. URL: [https://www-nds.iaea.org/exfor/servlet/X4sShowPubl?File=R_INDC\(CPR\)-16,1989](https://www-nds.iaea.org/exfor/servlet/X4sShowPubl?File=R_INDC(CPR)-16,1989).
- [43] Hauser, W., Feshbach, H., 1952. The inelastic scattering of neutrons. Phys. Rev. 87, 366–373. URL: <https://link.aps.org/doi/10.1103/PhysRev.87.366>, doi:[10.1103/PhysRev.87.366](https://doi.org/10.1103/PhysRev.87.366).
- [44] Helgesson, P., Sjöstrand, H., Rochman, D., 2017. Uncertainty-driven nuclear data evaluation including thermal (n, α) applied to ^{59}ni . Nuclear Data Sheets 145, 1–24. URL: <https://www.sciencedirect.com/science/article/pii/S0090375217300002>, doi:<https://doi.org/10.1016/j.nds.2017.09.001>.
- [45] Herman, M., Capote, R., Carlson, B., Oblozinsky, P., Sin, M., Trkov, A., Wienke, H., Zerkin, V., 2007. Empire: Nuclear reaction model code system for data evaluation. Nuclear Data Sheets 108, 2655–2715. URL: <https://www.sciencedirect.com/science/article/pii/S0090375207000001>, doi:<https://doi.org/10.1016/j.nds.2007.11.003>.
- [46] Hilaire, S., 2000. Statistical nuclear reactions. Workshop on Nuclear Data and Nuclear Reactors: Physics, Design and Safety, Trieste, 13 March - 14 April URL: https://inis.iaea.org/collection/NCLCollectionStore/_Public.
- [47] Igo, G., Thaler, R.M., 1957. Optical-model analysis of the elastic scattering of alpha particles. Phys. Rev. 106, 126–133. URL: <https://link.aps.org/doi/10.1103/PhysRev.106.126>, doi:[10.1103/PhysRev.106.126](https://doi.org/10.1103/PhysRev.106.126).
- [48] Ikeda, Y., Konno, C., Oishi, K., Nakamura, T., Miyade, H., Kawade, K., Yamamoto, H., Katoh, T., 1988. Activation cross section measurements on fusion reactor structural materials at neutron energy from 13.3 to 15.0 mev using fns facility. JAERI Reports No.1312 , 112URL: <https://doi.org/10.11484/jaeri-1312>.
- [49] Iwamoto, O., Nobuyuki Iwamoto, K.S., Ichihare, A., Kunieda, S., Minato, F., Nakayama, S., 2020. Status of jendl. EPJ Web Conf. 239, 09002. URL: <https://doi.org/10.1051/epjconf/202023909002>, doi:[10.1051/epjconf/202023909002](https://doi.org/10.1051/epjconf/202023909002).
- [50] James, F., Roos, M., 1975. Minuit: A System for Function Minimization and Analysis of the Parameter Errors and Correlations. Comput. Phys. Commun. 10, 343–367. doi:[10.1016/0010-4655\(75\)90039-9](https://doi.org/10.1016/0010-4655(75)90039-9).
- [51] Janka, H., Langanke, K., Marek, A., Martínez-Pinedo, G., Müller, B., 2007. Theory of core-collapse supernovae. Physics Reports 442, 38–74. URL: <https://www.sciencedirect.com/science/article/pii/S0370157307000000>, doi:<https://doi.org/10.1016/j.physrep.2007.02.002>. the Hans Bethe Centennial Volume 1906–2006.
- [52] Käppeler, F., Gallino, R., Bisterzo, S., Aoki, W., 2011. The s process: Nuclear physics, stellar models, and observations. Rev. Mod. Phys. 83, 157–193. URL: <https://link.aps.org/doi/10.1103/RevModPhys.83.157>, doi:[10.1103/RevModPhys.83.157](https://doi.org/10.1103/RevModPhys.83.157).
- [53] Kerlee, D.D., Blair, J.S., Farwell, G.W., 1957. Elastic scattering of alpha particles. Phys. Rev. 107, 1343–1362. URL: <https://link.aps.org/doi/10.1103/PhysRev.107.1343>, doi:[10.1103/PhysRev.107.1343](https://doi.org/10.1103/PhysRev.107.1343).
- [54] Khrumyleva, T., Bondarenko, I., Gurbich, A., Ketlerov, V., Khryachkov, V., Prusachenko, P., 2018. Investigation of (n, α) reaction cross sections for a number of structural material isotopes. Nuclear Science and Engineering 191, 282–290. doi:[10.1080/00295639.2018.1463746](https://doi.org/10.1080/00295639.2018.1463746).
- [55] Kneff, D., Oliver, B., Nakata, M., Farrar, H., 1981. Experimental helium generation cross sections for fast neutrons. Journal of Nuclear Materials 104, 1451–1455. URL: <https://www.sciencedirect.com/science/article/pii/0022311582908042>, doi:[https://doi.org/10.1016/0022-3115\(82\)90804-2](https://doi.org/10.1016/0022-3115(82)90804-2).
- [56] Koning, A., Delaroche, J., 2003. Local and global nucleon optical models from 1 kev to 200 mev. Nuclear Physics A 713, 231–310. URL: <https://www.sciencedirect.com/science/article/pii/S037594740201301>, doi:[https://doi.org/10.1016/S0375-9474\(02\)01321-0](https://doi.org/10.1016/S0375-9474(02)01321-0).
- [57] Koning, A., Duijvestijn, M., 2004. A global pre-equilibrium analysis from 7 to 200 mev based on the INDC(CPR)-16,1989 potential. Nuclear Physics A 744, 15–76. URL: <https://www.sciencedirect.com/science/article/pii/S0375947404008013>, doi:<https://doi.org/10.1016/j.nuclphysa.2004.08.013>.
- [58] Koning, A., Hilaire, S., Duijvestijn, M., 2008. Proceedings of the international conference on nuclear data for science and technology, april 22–27, 2007, nice, france, in: TALYS-1.0, EDP Sciences.
- [59] Koning, A., Hilaire, S., Goriely, S., 2019a. User Manual Talys-1.0, A nuclear reaction Program. URL: <http://www.talys.eu>.
- [60] Koning, A., Rochman, D., Sublet, J.C., Dzysiuk, N., Fleming, M., van der Marck, S., 2019b. TENDL: Complete Nuclear Data Library for Innovative Nuclear Science and Technology. Nuclear Data Sheets 155, 1–55. URL: <https://hal.archives-ouvertes.fr/hal-02008866>, doi:[10.1016/j.nds.2019.01.002](https://doi.org/10.1016/j.nds.2019.01.002).
- [61] Küçüksu, S., Yiğit, M., Paar, N., 2022. Statistical hauser-feshbach model description of (n, α) reaction cross sections for the weak s-process. Universe 8, 25. URL: <https://www.mdpi.com/2218-1997/8/1/25>, doi:<https://doi.org/10.3390/universe8010025>.
- [62] Levkovskii, V.N., Vinitskaya, G.P., Kovel'skaya, G.E., Stepanov, V.M., 1970. Cross sections for (n,p) and (n,α) reactions with 14.8-mev neutrons. Soviet Journal of Nuclear Physics 10, 25.
- [63] Lisboa, R., Malheiro, M., Alberto, P., 2004. The nuclear pseudospin symmetry along an isotopic chain. Brazilian Journal of Physics 34, 293–296.
- [64] Litvinova, E., Loens, H., Langanke, K., Martínez-Pinedo, G., Rauscher, T., Ring, P., Thielemann, F.K., Tselyaev, V., 2009. Low-lying dipole response in the relativistic quasiparticle

- time blocking approximation and its influence on neutron capture cross sections. Nuclear Physics A 823, 26–37. URL: <https://www.sciencedirect.com/science/article/pii/S0375947409001445>. doi:<https://doi.org/10.1016/j.nuclphysa.2009.03.009>.
- [65] Maenhaut, W., Adams, F., Hoste, J., 1973. Interferences in the determination of trace elements in high-purity tin. Journal of Radioanalytical and Nuclear Chemistry 16, 39–55.
- [66] Mannhart, W., Schmidt, D., 2007. Measurement of neutron activation cross sections in the energy range from 8 mev to 15 mev. PTB-N-53 38, 144S.
- [67] Meadows, J., Smith, D., Bretscher, M., Cox, S., 1987. Measurement of 14.7 mev neutron-activation cross sections for fusion. Annals of Nuclear Energy 14, 489–497. URL: <https://www.sciencedirect.com/science/article/pii/0306454987900661>. doi:[https://doi.org/10.1016/0306-4549\(87\)90066-1](https://doi.org/10.1016/0306-4549(87)90066-1).
- [68] Meadows, J., Smith, D., Greenwood, L., Haight, R., Ikeda, Y., Konno, C., 1996. Measurement of fast-neutron activation cross sections for copper, europium, hafnium, iron, nickel, silver, terbium and titanium at 10.0 and 14.7 mev and for the $be(d,n)$ thick-target spectrum. Annals of Nuclear Energy 23, 877–899. URL: <https://www.sciencedirect.com/science/article/pii/0306454995000682>. doi:[https://doi.org/10.1016/0306-4549\(95\)00068-2](https://doi.org/10.1016/0306-4549(95)00068-2).
- [69] Meadows, J.W., Smith, D.L., Greenwood, L.R., Geraldo, L.P., Mannhart, W., Börker, G., 1992. Measurements of the neutron cross section for $fe-54(n,\alpha)cr-51$ between 5.3 and 14.6 mev, in: Qaim, S.M. (Ed.), Nuclear Data for Science and Technology, Springer Berlin Heidelberg, Berlin, Heidelberg. pp. 288–290.
- [70] Mohr, P., Kiss, G., Fülop, Z., Galaviz, D., Gyürky, G., Somorjai, E., 2013. Elastic alpha scattering experiments and the alpha-nucleus optical potential at low energies. Atomic Data and Nuclear Data Tables 99, 651–679. URL: <https://www.sciencedirect.com/science/article/pii/S0092640X13000045>. doi:<https://doi.org/10.1016/j.adt.2012.10.003>.
- [71] Moldauer, P., 1980. Statistics and the average cross section. Nuclear Physics A 344, 185–195. URL: <https://www.sciencedirect.com/science/article/pii/0375947480906715>. doi:[https://doi.org/10.1016/0375-9474\(80\)90671-5](https://doi.org/10.1016/0375-9474(80)90671-5).
- [72] Moldauer, P.A., 1975. Why the hauser-feshbach formula works. Phys. Rev. C 11, 426–436. URL: <https://link.aps.org/doi/10.1103/PhysRevC.11.426>, doi:<https://doi.org/10.1103/PhysRevC.11.426>.
- [73] Molla, N., Qaim, S., 1977. A systematic study of (n, p) reactions at 14.7 mev. Nuclear Physics A 283, 269–288. URL: <https://www.sciencedirect.com/science/article/pii/037594747790436>. doi:[https://doi.org/10.1016/0375-9474\(77\)90431-6](https://doi.org/10.1016/0375-9474(77)90431-6).
- [74] Otuka, N., Dupont, E., Semkova, V., Pritychenko, B., Blokhin, A., Aikawa, M., Babykina, S., Bossant, M., Chen, G., Dunaeva, S., Forrest, R., Fukahori, T., Furutachi, N., Ganesan, S., Ge, Z., Gritzay, O., Herman, M., Hlavač, S., Katō, K., Lalremruata, B., Lee, Y., Makinaga, A., Matsumoto, K., Mikhaylyukova, M., Pikulina, G., Pronyaev, V., Saxena, A., Schwerer, O., Simakov, S., Soppera, N., Suzuki, R., Takács, S., Tao, X., Taova, S., Tárkányi, F., Varlamov, V., Wang, J., Yang, S., Zerkin, V., Zhuang, Y., 2014. Towards a more complete and accurate experimental nuclear reaction data library (exfor): International collaboration between nuclear reaction data centres (nrdc). Nuclear Data Sheets 120, 272–276. URL: <https://www.sciencedirect.com/science/article/pii/S0090375214005745>. doi:<https://doi.org/10.1016/j.nds.2014.07.065>.
- [75] Palumbo, A., Tan, W.P., Görres, J., Best, A., Couder, M., Crowter, R., deBoer, R.J., Falahat, S., LeBlanc, P.J., Lee, H.Y., O'Brien, S., Strandberg, E., Wiescher, M., Greene, J.P., Fülop, Z., Kiss, G.G., Somorjai, E., Özkan, N., Efe, G., Güray, R.T., 2012. Systematic study of the α -optical potential via elastic scattering near the $z = 50$ region for p -process nuclei. Phys. Rev. C 85, 035808. URL: <https://link.aps.org/doi/10.1103/PhysRevC.85.035808>, doi:<https://doi.org/10.1103/PhysRevC.85.035808>.
- [76] Paulsen, A., Widera, R., Arnotte, F., Liskien, H., 1979. Cross sections for the reactions $54fe(n, \alpha)51cr$, $54fe(n,p)54mn$, and $56fe(n,p)56mn$. Nuclear Science and Engineering 72, 113–116. URL: <https://doi.org/10.13182/NSE79-A19315>.
- [77] Pignatari, M., Gallino, R., Heil, M., Wiescher, M., Käppeler, F., Herwig, F., Bisterzo, S., 2010. The weak s-process in massive stars and its dependence on the neutron capture cross sections. The Astrophysical Journal 710, 1557–1577. URL: <https://doi.org/10.1088/0004-637x/710/2/1557>, doi:<https://doi.org/10.1088/0004-637x/710/2/1557>.
- [78] Plompen, A.J.M., Cabellos, O., De Saint Jean, C., Fleming, M., Algara, A., Angelone, M., Archier, P., Bauge, E., Bersillon, O., Blokhin, A., Cantargi, F., Chebboubi, A., Diez, C., Duarte, H., Dupont, E., Dyrda, J., Erasmus, B., Fiorito, L., Fischer, C., Kellett, M.A., Kim, D.H., Kim, H.I., Kodeli, I., Koning, A.J., Konobeyev, A.Y., Kopecky, S., Kos, B., Krásá, A., Leal, L.C., Leclaire, N., Leconte, P., Lee, Y.O., Leeb, H., Litaize, O., Majerle, M., Márquez Damián, J.I., Michel-Sendis, F., Mills, R.W., Morillon, B., Noguère, G., Pecchia, M., Pelloni, Pereslavtsev, P., Perry, R.J., Rochman, D., Röhrmoser, A., Romain, P., Romojaro, P., Roubtsov, D., Sauvan, P., Schillebeeckx, P., Schmidt, K.H., Serot, O., Simakov, S., Sirakov, I., Sjöstrand, H., Stankovskiy, A., Sublet, J.C., Tamagno, P., Trkov, A., van der Marck, S., Alvarez-Velarde, F., Villari, R., Ware, T.C., Yokoyama, K., Žerovník, G., 2020. The joint evaluated fission and fusion nuclear data library, jeff-3.3. European Physical Journal A 56, 181. URL: <https://doi.org/10.1140/epja/s10050-020-00141-9>, doi:<https://doi.org/10.1140/epja/s10050-020-00141-9>.
- [79] P.M.Gopych, M.N.Demchenko, I.M.Zalyubovskiy, P.S.Kizim, Th cross-sections of (n,α) reactions on $sn-112$, 114, 116 at the neutron energy 14.6 mev. Atomnaya Energiya 78, 329.
- [80] Praena, J., Sabaté-Gilarde, M., Porras, I., Quesada, J.M., Andrzejewski, J., Audouin, L., Bécaries, V., Barbagallo, M., Bečvář, F., Belloni, F., Berthoumieux, E., Billowes, J., Boccone, V., Bosnar, D., Brugger, M., Calviño, F., Calviani, M., Cano-Ott, D., Carrapico, C., Cerutti, F., Chiaveri, E., Chin, M., Colonna, N., Cortés, G., Cortés-Giraldo, M.A., Diakaki, M., Dietz, M., Domingo-Pardo, C., Dressler, R., Durán, I., Eleftheriadis, C., Ferrari, A., Fraval, K., Furman, V., Göbel, K., Gómez-Hornillos, M.B., Ganesan, S., García, Giubrone, G., Gonçalves, I.F., González-Romero, E., Goverdovski, A., Griesmayer, E., Guerrero, C., Gunsing, F., Heftrich, T., Hernández-Prieto, A., Heyse, J., Jenkins, D.G., Jericha, E., Käppeler, F., Kadi, Y., Karadimos, D., Katahuchi, T., Ketlerov, V., Khryachkov, V., Kivel, N., Koehler, P., Kokkoris, M., Kroll, J., Krčíčka, M., Lampoudis, C., Langer, C., Leal-Cidoncha, E., Lederer-Woods, C., Leeb, H., Leong, L.S., Lerendegui-Marco, J., Losito, R., Mallick, A., Manousos, A., Marganiec, J., Martínez, T., Massimi, C., Mastinu, P., Mastromarco, M., Mendoza, E., Mengoni, A., Milazzo, P.M., Mingrone, F., Mirea, M., Mondelaers, W., Paradela, C., Pavlik, A., Perkowski, J., Plompen, A.J.M., Rauscher, T., Reifarth, R., Riego-Perez, A., Robles, M., Rubbia, C., Ryan, J.A., Sarmento, R., Saxena, A., Schillebeeckx, P., Schmidt, S., Schumann, D., Sedyshev, P., Tagliente, G., Tain, J.L., Tarifeño Saldivia, A., Tarrío, D., Tassan-Got, L., Tsinganis, A., Valenta, S., Vannini, G., Variale, V., Vaz, P., Ventura, A., Vermeulen, M.J., Vlachoudis, V., Vlastou, R., Wallner, A., Ware, T., Weigand, M., Weiss, C., Wright, T., Zugec, P. (n_TOF Collaboration), 2018. Measurement and resonance analysis of the $^{33}S(n, \alpha)^{30}Si$ cross section at the cern n_tof facility in the energy region from 10 to 300 kev. Phys. Rev. C 97, 064603. URL: <https://link.aps.org/doi/10.1103/PhysRevC.97.064603>, doi:<https://doi.org/10.1103/PhysRevC.97.064603>.
- [81] Pritychenko, B., Mughaghbab, S., Sonzogni, A., 2010a. Calculations of maxwellian-averaged cross sections and astrophysical reaction rates using the endf/b-vii.0, jeff-3.1, jendl-3.3,

- and endf/b-vi.8 evaluated nuclear reaction data libraries. Atomic Data and Nuclear Data Tables 96, 645–748. URL: <https://www.sciencedirect.com/science/article/pii/S0092640X10000562>, doi:<https://doi.org/10.1016/j.adt.2010.05.002>.
- [82] Pritychenko, B., Mughaghab, S., Sonzogni, A., 2010b. Calculations of maxwellian-averaged cross sections and astrophysical reaction rates using the endf/b-vii.0, jeff-3.1, jendl-3.3, and endf/b-vi.8 evaluated nuclear reaction data libraries. Atomic Data and Nuclear Data Tables 96, 645–748. URL: <https://www.sciencedirect.com/science/article/pii/S0092640X10000562>, doi:<https://doi.org/10.1016/j.adt.2010.05.002>.
- [83] Pu, Z.S., Fan, K.K., Song, G.Q., 2011. Cross section measurements for (n, p) reaction on stannum isotopes at neutron energies from 13.5 to 14.6 MeV. Chinese Physics C 35, 445–448. URL: <https://doi.org/10.1088/1674-1137/35/5/007>, doi:<https://doi.org/10.1088/1674-1137/35/5/007>.
- [84] Rauscher, T., 2010. Relevant energy ranges for astrophysical reaction rates. Phys. Rev. C 81, 045807. URL: <https://link.aps.org/doi/10.1103/PhysRevC.81.045807>, doi:<https://doi.org/10.1103/PhysRevC.81.045807>.
- [85] Rauscher, T., Thielemann, F.K., 2000. Astrophysical reaction rates from statistical model calculations. Atomic Data and Nuclear Data Tables 75, 1–351. URL: <https://www.sciencedirect.com/science/article/pii/S0092640X00908B49>, Hernández-Prieto, A., Jenkins, D.G., Jericha, E., Kadi, Y., Käppeler, F., Karadimos, D., Kivel, N., Koehler, P., Kokkoris, M., Krtička, M., Kroll, J., Lampoudis, C., Langer, C., Leal-Cidoncha, E., Lederer, C., Leeb, H., Leong, L.S., Losito, R., Mallick, A., Manousos, A., Marganiec, J., Martínez, T., Massimi, C., Mastinu, P.F., Mastromarco, M., Meaze, M., Mendoza, E., Mengoni, A., Milazzo, P.M., Mingrone, F., Mirea, M., Mondalaers, W., Paradela, C., Pavlik, A., Perkowski, J., Plomp, A., Praena, J., Quesada, J.M., Rauscher, T., Reifarth, R., Riego, A., Robles, M.S., Roman, F., Rubbia, C., Sabaté-Gilarte, M., Sarmento, R., Saxena, A., Schillebeeckx, P., Schmidt, S., Schumann, D., Tagliente, G., Tain, J.L., Tarrío, D., Tassan-Got, L., Tsinganis, A., Valenta, S., Vannini, G., Variale, V., Vaz, P., Ventura, A., Versaci, R., Vermeulen, M.J., Vlachoudis, V., Vlastou, R., Wallner, A., Ware, T., Weigand, M., Wright, T., Žugec, P., 2013. A new cvd diamond mosaic-detector for (n, α) cross-section measurements at the n_tof experiment at cern. Nuclear Instruments and Methods in Physics Research Section A: Accelerators, Spectrometers, Detectors and Associated Equipment 732, 190–194. URL: <https://www.sciencedirect.com/science/article/pii/S0168900213010040>, doi:<https://doi.org/10.1016/j.nima.2013.07.040>.
- [86] Sabaté-Gilarte, M., Praena, J., Porras, I., Quesada, J., Mastinu, P., 2016. Measurement of the $^{33}\text{S}(n, \alpha)$ cross-section at n_tof(cern): Applications to bnct. Reports of Practical Oncology & Radiotherapy 21, 113–116. URL: <https://www.sciencedirect.com/science/article/pii/S150713671400145X>, doi:<https://doi.org/10.1016/j.rpor.2014.08.007>.
- [87] Salisbury, S.R., Chalmers, R.A., 1965. $\text{fe}^{54}(n, p)$, (n, α) , $(n, 2n)$ cross sections. Phys. Rev. 140, B305–B310. URL: <https://link.aps.org/doi/10.1103/PhysRev.140.B305>, doi:<https://doi.org/10.1103/PhysRev.140.B305>.
- [88] Saraf, S.K., Brient, C.E., Egún, P.M., Grimes, S.M., Mishra, V., Pedroni, R.S., 1991. Cross sections and spectra for the ^{54}Fe and ^{56}Fe (n, xp) and $(n, x\alpha)$ reactions between 8 and 15 mev. Nuclear Science and Engineering 107, 365–373. URL: <https://doi.org/10.13182/NSE88-120>, doi:<https://doi.org/10.13182/NSE88-120>.
- [89] Shibata, K., Iwamoto, O., Nakagawa, T., Iwamoto, N., Ichihara, A., Kunieda, S., Chiba, S., Furutaka, K., Otuka, N., Ohsawa, T., Murata, T., Matsunobu, H., Zukeran, A., Kamada, S., ichi Kataura, J., 2011. Jendl-4.0: A new library for nuclear science and engineering. Journal of Nuclear Science and Technology 48, 1–30. URL: <https://doi.org/10.1080/18811248.2011.9711675>, doi:<https://doi.org/10.1080/18811248.2011.9711675>.
- [90] Shibata, K., Kawano, T., Nakagawa, T., Iwamoto, O., ichi Kataura, J., Fukahori, T., Chiba, S., Hasegawa, A., Murata, T., Matsunobu, H., Ohsawa, T., Nakajima, Y., Yoshida, T., Zukeran, A., Kawai, M., Baba, M., Ishikawa, M., Asami, T., Watanabe, T., Watanabe, Y., Igashira, M., Yamamuro, N., Kitazawa, H., Yamano, N., Takano, H., 2002. Japanese evaluated nuclear data library version 3 revision-3: Jendl-3.3. Journal of Nuclear Science and Technology 39, 1125–1136. doi:<https://doi.org/10.1080/18811248.2002.9715303>.
- [91] Sterbenz, S.M., Bateman, F.B., Lee, T.M., Haight, R.C., Young, P.G., Chadwick, M.B., Goeckner, F.C., Brient, C.E., Grimes, S.M., Maier-Komor, P., Vonach, H., 1994. The $^{56}\text{Fe}(n, \alpha)$ reaction from threshold to 30 mev. American Nuclear Society 1, 314.
- [92] Thielemann, F.K., Arcones, A., Käppeli, R., Liebendörfer, M., Rauscher, T., Winteler, C., Fröhlich, C., Dillmann, I., Fischer, T., Martinez-Pinedo, G., Langanke, K., Farouqi, K., Kratz, K.L., Panov, I., Korneev, I.K., 2011. What are the astrophysical sites for the r-process and the production of heavy elements? Progress in Particle and Nuclear Physics 66, 346–353. URL: <https://www.sciencedirect.com/science/article/pii/S0146641011000020>, doi:<https://doi.org/10.1016/j.ppnp.2011.01.032>.
- [93] Vermote, S., Wagemans, C., De Smet, L., Lampoudis, C., Van Gils, J., 2012. Experimental determination of the $^{41}\text{Ca}(n, \alpha)^{38}\text{Ar}$ reaction cross section up to 80 kev, and calculation of the maxwellian averaged cross section at stellar temperatures. Phys. Rev. C 85, 015803. URL: <https://link.aps.org/doi/10.1103/PhysRevC.85.015803>, doi:<https://doi.org/10.1103/PhysRevC.85.015803>.
- [94] Wang, Z., Fan, X., Zhang, L., Bai, H., Chen, J., Zhang, G., Gledenov, Y.M., Sedysheva, M.V., Krupa, L., Khuukhenkhuu, G., 2012. Cross sections of the $^{56}\text{Fe}(n, \alpha)^{53}\text{Cr}$ and $^{54}\text{Fe}(n, \alpha)^{51}\text{Cr}$ reactions in the mev region. Phys. Rev. C 92, 044601. URL: <https://link.aps.org/doi/10.1103/PhysRevC.92.044601>, doi:<https://doi.org/10.1103/PhysRevC.92.044601>.
- [95] Weiß, C., Griesmayer, E., Guerrero, C., Altstadt, S., Andrzejewski, J., Audouin, L., Badurek, G., Barbagallo, M., Bécaries, V., Bečvář, F., Belloni, F., Berthoumieux, E., Billowes, J., Boccone, V., Bosnar, D., Brugger, M., Calviani, M., Calviño, F., Cano-Ott, D., Carrapiço, C., Cerutti, F., Chiaveri, E., Chin, M., Colonna, N., Cortés, G., Cortés-Giraldo, M.A., Diakaki, M., Domingo-Pardo, C., Duran, I., Dressler, R., Dzysiuk, N., Eleftheriadis, C., Ferrari, A., Fraval, K., Ganesan, S., García, A.R., Giubrone, G., Gómez-Hornillos, M.B., Gonçalves, I.F., González-Romero, E., Gunsing, F., Gurusamy, P., Hernández-Prieto, A., Jenkins, D.G., Jericha, E., Kadi, Y., Käppeler, F., Karadimos, D., Kivel, N., Koehler, P., Kokkoris, M., Krtička, M., Kroll, J., Lampoudis, C., Langer, C., Leal-Cidoncha, E., Lederer, C., Leeb, H., Leong, L.S., Losito, R., Mallick, A., Manousos, A., Marganiec, J., Martínez, T., Massimi, C., Mastinu, P.F., Mastromarco, M., Meaze, M., Mendoza, E., Mengoni, A., Milazzo, P.M., Mingrone, F., Mirea, M., Mondalaers, W., Paradela, C., Pavlik, A., Perkowski, J., Plomp, A., Praena, J., Quesada, J.M., Rauscher, T., Reifarth, R., Schumann, D., Tagliente, G., Tain, J.L., Tarrío, D., Tassan-Got, L., Tsinganis, A., Valenta, S., Vannini, G., Variale, V., Vaz, P., Ventura, A., Versaci, R., Vermeulen, M.J., Vlachoudis, V., Vlastou, R., Wallner, A., Ware, T., Weigand, M., Wright, T., Žugec, P., 2014. The (n, α) reaction in the s-process

- branching point ^{59}ni . Nuclear Data Sheets 120, 208–210. URL:
<https://www.sciencedirect.com/science/article/pii/S0090375214005006>,
doi:<https://doi.org/10.1016/j.nds.2014.07.048>.
- [97] Yu, Y.W., Gardner, D.G., 1967. Cross sections of some reactions of ar, ti, ni, cd and pb with 14.1 mev neutrons. Nuclear Physics A 98, 451–459. URL:
<https://www.sciencedirect.com/science/article/pii/0375947467900917>,
doi:[https://doi.org/10.1016/0375-9474\(67\)90091-7](https://doi.org/10.1016/0375-9474(67)90091-7).
- [98] Zabrodskaya, S.V., Ignatyuk, A.V., Koshcheev, V.N., Manokhin, V.N., Nikolaev, M.N., Pronyaev, G.V., 2007. Russian national library of evaluated neutron data. VANT. Ser.: Nuclear and Reactor Constants 12, 3–21.
- [99] Zelenetskij, A.V., 1995. Investigation of isotopic dependence of (n,α) reaction cross sections at neutron energy $e_n = 14.5$ mev. Izvestiya Vysshikh Uchebnykh Zavedenij Yadernaya Ehnergetika 6, 44–49. URL:
http://inis.iaea.org/search/search.aspx?orig_q=RN:28078989.